General Method for the Selective Functionalization of Cyclopentadienyliron Tricarbadecaboranyl Complexes via Halogenation and Sonogashira Coupling Reactions

Robert Butterick III, Patrick J. Carroll, and Larry G. Sneddon*

Department of Chemistry, University of Pennsylvania, Philadelphia, Pennsylvania 19104-6323

Received May 2, 2008

A general method for the selective functionalization of cyclopentadienyliron tricarbadecaboranyl complexes has been developed that employs selective halogenation of the tricarbadecaboranyl ligand followed by Sonogashira coupling reactions. The reaction of *N*-chloro (NCS) or *N*-bromosuccinimide (NBS) with 1-(η^5-C_5H_5)-2-Ph-*closo*-1,2,3,4-$FeC_3B_7H_9$ (**2**) resulted in selective halogenation at the B6-boron of the tricarbadecaboranyl ligand to form 1-(η^5-C_5H_5)-2-Ph-6-X-*closo*-1,2,3,4-$FeC_3B_7H_8$ (X = Cl (**3**), Br (**4**)), respectively. **4** was also formed selectively by the reaction of **2** with Br_2. The $AlCl_3$-catalyzed reaction of **2** with ICl gave an easily separated mixture of 1-(η^5-C_5H_5)-2-Ph-6-I-*closo*-1,2,3,4-$FeC_3B_7H_8$ (**5**), 1-(η^5-C_5H_5)-2-Ph-11-I-*closo*-1,2,3,4-$FeC_3B_7H_8$ (**6**), and 1-(η^5-C_5H_5)-2-Ph-6-I-11-I-*closo*-1,2,3,4-$FeC_3B_7H_7$ (**7**). Reaction of **5** with terminal acetylenes in the presence of $(PPh_3)_2PdCl_2$/CuI in Et_2NH solvent yielded a series of acetylene-functionalized metallatricarbadecaboranyl complexes, 1-(η^5-C_5H_5)-2-Ph-6-(RC≡C)-*closo*-1,2,3,4-$FeC_3B_7H_8$ (R = Ph (**8**), $(CH_3)_3Si$ (**9**), $CH_2OC(O)CH_2CH_3$ (**11**), (η^5-C_5H_4)Fe(η^5-C_5H_5) (**12**)). **9** reacted with fluoride ion to give the deprotected acetylene complex 1-(η^5-C_5H_5)-2-Ph-6-(HC≡C)-*closo*-1,2,3,4-$FeC_3B_7H_8$ (**10**). The structures of **3**−**12** have been crystallographically determined.

Introduction

Owing to their potential uses in a range of medical, optical, and electronic applications, metallocenes have been one of the most extensively studied classes of organometallic complexes. For example, many metallocenes, such as (η^5-C_5H_5)$_2MX_2$ (M = Ti, V, Nb, Mo, and W) and [(η^5-C_5H_5)$_2$Fe]$^+X^-$, and their functionalized derivatives (e.g., hydroxyferrocifens), have potent antitumor properties.[1] Other metallocenes, such as ferrocene and ruthenocene, have been employed as components of electron-transfer and nonlinear optical materials.[2]

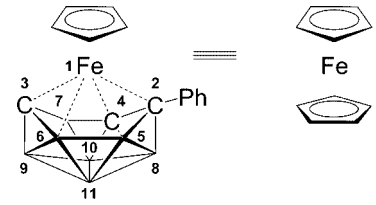

Figure 1. Comparison of the structures of 1-(η^5-C_5H_5)-2-Ph-*closo*-1,2,3,4-$FeC_3B_7H_9$ (**2**) and ferrocene.

We have previously shown[3] that, owing to their similar charge and electron-donating abilities, the tricarbadecaboranide anions 6-R-5,6,9-*nido*-$C_3B_7H_9^-$ (R = Me or Ph) have coordination properties that are in many ways similar to those of the cyclopentadienide $C_5H_5^-$ anion (Figure 1). However, the derived metallatricarbadecaboranyl complexes have properties, including enhanced oxidative and hydrolytic stabilities and substantially different electrochemical and chemical activities, that are quite distinct from their metallocene analogues. These differences could have important advantages in many applications. For example, we have shown that cationic cyclopentadienyliron tricarbadecaboranyl complexes[4] and vanada- and niobatricarbadecaboranyl halide complexes[5] not only are air and moisture stable but also exhibit potent cytotoxic activities against suspended tumor cells that complement those of the corresponding metallocenes.

Further utilization of metallatricarbadecaboranyl complexes for biomedical or materials applications now requires the development of new methods for their systematic functional-

* Corresponding author. E-mail: lsneddon@sas.upenn.edu.

(1) (a) Neuse, E. W. *J. Inorg. Organomet. Polym.* **2005**, *15*, 3–32. (b) Köpf-Maier, P.; Köpf, H. *Chem. Rev.* **1987**, *87*, 1137–1152. (c) Köpf-Maier, P.; Köpf, H. *Struct. Bonding (Berlin)* **1988**, 103–185. (d) Köpf-Maier, P.; Köpf, H. *Met. Comp. Cancer Ther.* **1994**, 109–146. (e) Kuo, L. Y.; Liu, A. H.; Marks, T. J. *Met. Ions Biol. Syst.* **1996**, *33*, 53–85. (f) Harding, M. M.; Mokdsi, G. *Curr. Med. Chem.* **2000**, *7*, 1289–1303. (g) Guo, Z.; Sadler, P. J. *Adv. Inorg. Chem.* **2000**, *49*, 183–306. (h) Vessières, A.; Top, S.; Beck, W.; Hillard, E.; Jaouen, G. *Dalton Trans.* **2006**, 529–541.

(2) Barlow, S.; Marder, S. R. *Chem. Commun.* **2000**, 1555–1562.

(3) (a) Plumb, C. A.; Carroll, P. J.; Sneddon, L. G. *Organometallics* **1992**, *11*, 1665–1671. (b) Plumb, C. A.; Carroll, P. J.; Sneddon, L. G. *Organometallics* **1992**, *11*, 1672–1680. (c) Barnum, B. A.; Carroll, P. J.; Sneddon, L. G. *Organometallics* **1996**, *15*, 645–654. (d) Weinmann, W.; Wolf, A.; Pritzkow, H.; Siebert, W.; Barnum, B. A.; Carroll, P. J.; Sneddon, L. G. *Organometallics* **1995**, *14*, 1911–1919. (e) Barnum, B. A.; Carroll, P. J.; Sneddon, L. G. *Inorg. Chem.* **1997**, *36*, 1327–1337. (f) Müller, T.; Kadlecek, D. E.; Carroll, P. J.; Sneddon, L. G.; Siebert, W. *J. Organomet. Chem.* **2000**, *614*−*615*, 125–130. (g) Wasczcak, M. D.; Wang, Y.; Garg, A.; Geiger, W. E.; Kang, S. O.; Carroll, P. J.; Sneddon, L. G. *J. Am. Chem. Soc.* **2001**, *123*, 2783–2790. (h) Ramachandran, B. M.; Carroll, P. J.; Sneddon, L. G. *Inorg. Chem.* **2004**, *43*, 3467–3474. (i) Ramachandran, B. M.; Carroll, P. J.; Sneddon, L. G. *J. Am. Chem. Soc.* **2000**, *122*, 11033–11034. (j) Ramachandran, B. M.; Trupia, S. M.; Geiger, W. E.; Carroll, P. J.; Sneddon, L. G. *Organometallics* **2002**, *21*, 5078–5090. (k) Butterick, R.; Ramachandran, B. M.; Carroll, P. J.; Sneddon, L. G. *J. Am. Chem. Soc.* **2006**, *128*, 8626–8637. (l) Nafady, A.; Butterick, R.; Calhorda, M. J.; Carroll, P. J.; Chong, D.; Geiger, W. E.; Sneddon, L. G. *Organometallics* **2007**, *26*, 4471–4482.

(4) Wasczcak, M. D.; Lee, C. C.; Hall, I. H.; Carroll, P. J.; Sneddon, L. G. *Angew. Chem., Int. Ed. Engl.* **1997**, *36*, 2228–2230.

(5) Hall, I. H.; Durham, R.; Tran, M.; Mueller, S.; Ramachandran, B. M.; Sneddon, L. G. *J. Inorg. Biochem.* **2003**, *93*, 125–131.

10.1021/om8003898 CCC: $40.75
Publication on Web 08/09/2008

ization to allow the syntheses of more complex derivatives with, for example, the chemically reactive groups needed for selective tumor binding or the conjugation-linked push−pull groups needed for electronic and optical materials. In response to this need, we report here a general method for the direct functionalization of cyclopentadienyliron tricarbadecaboranyl complexes via selective cage-halogenation and subsequent Sonogashira coupling reactions.

Experimental Section

General Synthetic Procedures and Material. Unless otherwise noted, all reactions and manipulations were performed in dry glassware under a nitrogen or argon atmosphere using the high-vacuum or inert-atmosphere techniques described by Shriver.[6]

The $Li^+[6\text{-Ph-}nido\text{-}5,6,9\text{-}C_3B_7H_9^-]$ (**1**$^-$)[3h] and 1-(η^5-C_5H_5)-2-Ph-*closo*-1,2,3,4-$FeC_3B_7H_9$ (**2**)[3j] were prepared by the reported methods. *N*-Chlorosuccinimide, *N*-bromosuccinimide, bromine, iodine monochloride, aluminum chloride, $(C_6H_5)_3P$, phenylacetylene, ethynylferrocene, propargyl proprionate, diethyl amine (Aldrich), trimethylsilylacetylene (Lancaster), bis(benzonitrile)palladium(II) chloride, CuI (Strem), spectrochemical grade dichloromethane, and hexanes (Fisher) were used as received. Glyme and THF (Fisher) were freshly distilled from sodium-benzophenone ketyl, and carbon disulfide (Fisher) was freshly distilled from calcium hydride prior to use. All other solvents were used as received unless noted otherwise.

Physical Methods. ^{11}B NMR at 128.4 MHz and ^{1}H NMR at 400.1 MHz were obtained on a Bruker DMX-400 spectrometer equipped with appropriate decoupling accessories. All ^{11}B chemical shifts are referenced to $BF_3 \cdot OEt_2$ (0.0 ppm), with a negative sign indicating an upfield shift. All proton chemical shifts were measured relative to internal residual protons from the lock solvents (99.9% CD_2Cl_2), then referenced to $(CH_3)_4Si$ (0.0 ppm). NMR data are summarized in Table 1. High- and low-resolution mass spectra employing chemical ionization with negative ion detection were obtained on a Micromass AutoSpec high-resolution mass spectrometer. IR spectra were obtained on a Perkin-Elmer Spectrum 100 FT-IR spectrometer. Elemental analyses were carried out at Robertson Microlit Laboratories in Madison, NJ. Melting points were determined using a standard melting point apparatus and are uncorrected.

1-(η^5-C_5H_5)-2-Ph-6-Cl-*closo*-1,2,3,4-$FeC_3B_7H_8$ (3). A solution of **2** (200 mg, 0.63 mmol) and *N*-chlorosuccinimide (126 mg, 0.94 mmol) in CH_2Cl_2 (10 mL) was stirred at room temperature for 18 h. The blue solution was then exposed to air and filtered through a short plug of silica using CH_2Cl_2 as the eluent. The solvent was evaporated from the filtrate to yield a dark blue powder. For **3**: 1-(η^5-C_5H_5)-2-Ph-6-Cl-*closo*-1,2,3,4-$FeC_3B_7H_8$, 52% yield (116 mg, 0.33 mmol); dark blue; mp 198 °C. HRMS: *m/z* calcd for $^{12}C_{14}{}^1H_{18}{}^{11}B_7{}^{35}Cl^{56}Fe^-$ 354.1098, found 354.1110. ^{11}B NMR (128.4 MHz, CD_2Cl_2, ppm, J = Hz): 4.3 (d, 158, 1B), −1.0 (overlapped d/s, broad, 2B), −10.6 (d, 150, 1B), −25.5 (d, 153, 1B), −27.3 (d, 169, 1B), −36.4 (d, 161, 1B). ^{1}H NMR (400.1 MHz, CD_2Cl_2, ppm, J = Hz): 7.49−8.62 (Ph), 6.78 (dd (7, 5), C3H), 4.53 (s, Cp), 1.80 (s, C4H). IR (KBr, cm^{-1}): 3105 (s), 3055 (s), 2570 (vs, br), 1956 (m), 1891 (m), 1807 (m), 1713 (w, br), 1598 (m), 1580 (m), 1497 (s), 1446 (s), 1426 (s), 1127 (s, br).

1-(η^5-C_5H_5)-2-Ph-6-Br-*closo*-1,2,3,4-$FeC_3B_7H_8$ (4). A solution of **2** (200 mg, 0.63 mmol) and *N*-bromosuccinimide (167 mg, 0.94 mmol) in CH_2Cl_2 (10 mL) was stirred at room temperature for 18 h. The blue solution was then exposed to air and filtered through a short plug of silica using CH_2Cl_2 as the eluent. The solvent was evaporated from the filtrate to yield a dark blue powder. For **4**: 1-(η^5-C_5H_5)-2-Ph-6-Br-*closo*-1,2,3,4-$FeC_3B_7H_8$, 95% yield (237 mg, 0.60 mmol); dark blue; mp 196 °C; Anal. Calcd: C, 42.28, H, 4.56. Found: C, 41.89, H, 4.45. HRMS: *m/z* calcd for $^{12}C_{14}{}^1H_{18}{}^{11}B_7{}^{79}Br^{56}Fe^-$ 398.0593, found 398.0576. ^{11}B NMR (128.4 MHz, $CDCl_3$, ppm, J = Hz): 4.4 (d, 156, 1B), −0.2 (d, 171, 1B), −6.9 (s, 1B), −10.1 (d, 150, 1B), −24.9 (d, 150, 1B), −26.9 (d, 159, 1B), −35.3 (d, 162, 1B). ^{1}H NMR (400.1 MHz, $CDCl_3$, ppm, J = Hz): 7.44−8.65 (Ph), 6.90 (dd (6, 5), C3H), 4.54 (s, Cp), 1.79 (s, C4H). IR (KBr, cm^{-1}): 3103 (s), 3053 (s), 2922 (m), 2851 (w), 2568 (vs, br), 1957 (m), 1891 (m, br), 1809 (m), 1712 (w), 1597 (m), 1580 (m), 1497 (s), 1446 (s), 1426 (s), 1312 (m), 1214 (m), 1119 (s, br).

Alternate Synthesis of 4. A CH_2Cl_2 solution of Br_2 (3.0 mL of a 1.0 M solution, 3.0 mmol) was added dropwise to a stirring CH_2Cl_2 (10 mL) solution of **2** (500 mg, 1.57 mmol) at room temperature in air, resulting in immediate bubbling. After stirring for 5 min at room temperature, the solution was filtered through a short plug of silica using CH_2Cl_2 as the eluent. The solvent was evaporated from the filtrate to yield a dark blue powder. This material, obtained in 81% yield (504 mg, 1.27 mmol), was identified by its ^{11}B NMR, ^{1}H NMR, mass spectrum, and melting point.

Reaction of 2 and ICl/AlCl$_3$. A CH_2Cl_2 solution of ICl (4.7 mL of a 1.0 M solution, 4.7 mmol) was added dropwise to a stirring CS_2 (20 mL) solution of **2** (300 mg, 0.94 mmol) and $AlCl_3$ (138 mg, 1.04 mmol) under N_2. Stirring was continued at room temperature for 65 h. The solvent was removed *in vacuo*, and the dark blue residue was dissolved in 30 mL of CH_2Cl_2 and washed with 2 × 25 mL of $Na_2S_2O_3$ solution (0.8 M in H_2O) followed by 3 × 25 mL of H_2O. The organic layer was then dried with $MgSO_4$ and filtered through a short plug of silica using CH_2Cl_2 as the eluent. The solvent was evaporated from the filtrate to yield a dark blue, oily material. A silica column separation using 3:1 hexanes/CH_2Cl_2 as the eluent gave four well-separated bands: (1) unreacted **2**, 6% recovery (19 mg, 0.06 mmol); (2) **1-(η^5-C_5H_5)-2-Ph-6-I-*closo*-**1,2,3,4-$FeC_3B_7H_8$ (**5**), 44% yield (184 mg, 0.41 mmol); dark blue; mp 203 °C. Anal. Calcd: C, 37.81, H, 4.08. Found: C, 39.03, H, 4.03. HRMS: *m/z* calcd for $^{12}C_{14}{}^1H_{18}{}^{11}B_7{}^{56}Fe^{127}I^-$ 446.0454, found 446.0455. ^{11}B NMR (128.4 MHz, CD_2Cl_2, ppm, J = Hz): 3.9 (d, 153, 1B), 0.8 (d, 158, 1B), −9.7 (d, 157, 1B), −21.7 (s, 1B), −24.3 (d, 150, 1B), −27.1 (d, 160, 1B), −33.0 (d, 155, 1B). ^{1}H NMR (400.1 MHz, CD_2Cl_2, ppm, J = Hz): 7.44−8.64 (Ph), 6.99 (dd (6, 5), C3H), 4.56 (s, Cp), 1.91 (C4H). IR (KBr, cm^{-1}) 3101 (m), 3047 (s), 2562 (vs, br), 1957 (m), 1887 (m, br), 1810 (m, br), 1596 (m), 1579 (m), 1497 (s), 1445 (s), 1426 (s), 1311 (m), 1213 (m), 1118 (s, br); (3) **1-(η^5-C_5H_5)-2-Ph-11-I-*closo*-**1,2,3,4-$FeC_3B_7H_8$ (**6**), 8% yield (34 mg, 0.08 mmol); dark blue; mp 198 °C. Anal. Calcd: C, 37.81, H, 4.08. Found: C, 37.80, H, 3.99. HRMS: *m/z* calcd for $^{12}C_{14}{}^1H_{18}{}^{11}B_7{}^{56}Fe^{127}I^-$ 446.0454, found 446.0444. ^{11}B NMR (128.4 MHz, CD_2Cl_2, ppm, J = Hz): 4.6 (d, 158, 1B), 1.4 (d, 155, 1B), −9.4 (d, 142, 1B), −10.2 (d, 131, 1B), −26.4 (d, 165, 1B), −29.4 (s, 1B), −31.7 (d, 159, 1B). ^{1}H NMR (400.1 MHz, CD_2Cl_2, ppm, J = Hz): 7.45−8.60 (Ph), 6.88 (m, C3H), 4.52 (s, Cp), 1.90 (s, C4H). IR (KBr, cm^{-1}) 3107 (m), 3040 (s), 2962 (m), 2926 (m), 2855 (w), 2588 (vs), 2568 (vs), 2533 (vs), 1983 (w), 1963 (w), 1896 (w, br), 1867 (w), 1812 (m, br), 1698 (m, br), 1598 (m), 1578 (m), 1497 (s), 1446 (s), 1424 (s), 1310 (m), 1263 (m), 1207 (m), 1119 (s, br); (4) **1-(η^5-C_5H_5)-2-Ph-6-I-11-I-*closo*-1,2,3,4-$FeC_3B_7H_7$** (**7**), 11% yield (57 mg, 0.10 mmol); dark blue; mp >300 °C. Anal. Calcd: C, 29.47, H, 3.00. Found: C, 29.80, H, 2.80. HRMS: *m/z* calcd for $^{12}C_{14}{}^1H_{17}{}^{11}B_7{}^{56}Fe^{127}I_2^-$ 571.9420, found 571.9418. ^{11}B NMR (128.4 MHz, CD_2Cl_2, ppm, J = Hz): 5.4 (d, 170, 1B), 1.6 (d, 178, 1B), −8.5 (d, 150, 1B),.−20.2 (s, 1B) −25.3 (d, 161, 1B), −27.9 (s, 1B), −31.3 (d, 165, 1B). ^{1}H NMR (400.1 MHz, CD_2Cl_2, ppm, J = Hz): 7.43−8.61 (Ph), 6.99 (dd (7, 5), C3H), 4.62 (s, Cp), 2.01 (s, C4H). IR (KBr, cm^{-1}): 3100 (m), 3054 (s), 2925 (w), 2611 (vs), 2560 (vs, br), 1979 (w), 1958 (w), 1905 (w), 1885 (w),

(6) Shriver, D. F.; Drezdzon, M. A. *The Manipulation of Air-Sensitive Compounds*, 2nd ed.; Wiley: New York, 1986.

Table 1. Crystallographic Data Collection and Structure Refinement Information

	3	**4**	**5**	**6**	**7**	**8**	**9**	**10**	**11**	**12**
empirical formula	$C_{14}H_{18}B_7ClFe$	$C_{14}H_{18}B_7BrFe$	$C_{14}H_{18}B_7FeI$	$C_{14}H_{18}B_7FeI$	$C_{14}H_{17}B_7FeI_2$	$C_{22}H_{23}B_7Fe$	$C_{18}H_{24}B_7FeSi$	$C_{16}H_{19}B_7Fe$	$C_{20}H_{25}B_7FeO_2$	$C_{26}H_{27}B_7Fe_2$
fw	353.25	397.71	444.70	444.70	570.60	418.92	399.98	342.83	428.92	526.85
cryst class	monoclinic	monoclinic	monoclinic	monoclinic	orthorhombic	orthorhombic	orthorhombic	monoclinic	monoclinic	orthorhombic
space group	$P2_1/n$ (#14)	$P2_1/n$ (#14)	$P2_1/n$ (#14)	$P2_1/c$ (#14)	*Pbca* (#61)	*Pbca* (#61)	*Pbca* (#61)	$P2_1/n$ (#14)	$C2/c$ (#15)	*Pbca* (#61)
Z	4	4	4	4	8	8	8	4	8	8
a, Å	12.0508(9)	12.106(5)	12.1284(9)	7.9101(8)	10.0586(7)	12.0350(10)	12.5475(9)	11.3970(17)	26.301(5)	13.2209(9)
b, Å	10.2933(5)	10.352(9)	10.4889(7)	21.471(2)	19.0567(13)	15.3761(14)	14.5849(11)	11.0532(15)	8.0268(11)	15.8060(11)
c, Å	13.7372(8)	13.838(7)	14.0174(11)	10.4106(10)	19.9757(14)	22.1162(17)	23.4740(17)	13.4141(19)	20.940(3)	22.9420(16)
β, deg	107.224(3)	106.343(6)	104.939(2)	105.810(2)				100.375(3)	109.861(4)	
V, Å^3	1627.6(2)	1664(2)	1722.9(2)	1701.2(3)	3829.0(5)	4092.6(6)	4295.8(5)	1662.2(4)	4157.7(11)	4794.2(6)
D_{calc}, g/cm^3	1.442	1.588	1.714	1.736	1.980	1.360	1.237	1.370	1.370	1.460
μ, cm^{-1}	10.78	32.95	26.56	26.89	40.05	7.44	7.58	8.98	7.40	12.25
λ, Å (Mo Kα)	0.71069	0.71069	0.71069	0.71073	0.71073	0.71073	0.71073	0.71073	0.71073	0.71073
cryst size, mm	0.32 × 0.30 × 0.10	0.28 × 0.22 × 0.06	0.30 × 0.28 × 0.01	0.35 × 0.25 × 0.20	0.30 × 0.15 × 0.05	0.25 × 0.09 × 0.02	0.42 × 0.20 × 0.01	0.44 × 0.35 × 0.10	0.48 × 0.35 × 0.24	0.38 × 0.30 × 0.12
F(000)	720	792	864	864	2144	1728	1656	704	1776	2160
2θ angle, deg	5.02−54.96	5.26−54.96	5.14−54.92	5.36−55.02	5.02−55.00	5.00−50.02	5.52−50.04	5.18−54.92	5.34−54.98	5.16 − 54.94
temperature, K	143	143	143	143	143	143	143	143	143	143
hkl collected	$-11 \le h \le 15$; $-5 \le k \le 13$; $-17 \le l \le 17$	$-14 \le h \le 15$; $-10 \le k \le 13$; $-17 \le l \le 17$	$-15 \le h \le 12$; $-13 \le k \le 13$; $-18 \le l \le 18$	$-9 \le h \le 10$; $-22 \le k \le 27$; $-13 \le l \le 13$	$-13 \le h \le 10$; $-24 \le k \le 24$; $-25 \le l \le 24$	$-12 \le h \le 14$; $-18 \le k \le 16$; $-26 \le l \le 25$	$-14 \le h \le 13$; $-13 \le k \le 17$; $-27 \le l \le 25$	$-14 \le h \le 14$; $-14 \le k \le 14$; $-17 \le l \le 14$	$-33 \le h \le 33$; $-9 \le k \le 10$; $-26 \le l \le 27$	$-17 \le h \le 16$; $-20 \le k \le 15$; $-29 \le l \le 24$
no. of reflns measd	9201	12 370	17 210	10 019	38 636	17 504	17 367	12 840	24 154	30 071
no. of unique reflns	3594 (R_{int} = 0.0250)	3801 (R_{int} = 0.0198)	3916 (R_{int} = 0.0348)	3851 (R_{int} = 0.0211)	4371 (R_{int} = 0.0303)	3601 (R_{int} = 0.0502)	3780 (R_{int} = 0.0380)	3788 (R_{int} = 0.0302)	4738 (R_{int} = 0.0208)	5448 (R_{int} = 0.0269)
no. of obsd reflns ($F > 4\sigma$)	3205	3408	3536	3469	4018	2728	3041	3250	4514	4800
no. of reflns used in refinement	3594	3801	3916	3851	4371	3601	3780	3788	4738	5448
no. of params	281	241	242	241	245	304	289	294	305	349
R^a indices ($F > 4\sigma$)	R_1 = 0.0421 wR_2 = 0.1068	R_1 = 0.0353 wR_2 = 0.0813	R_1 = 0.0388 wR_2 = 0.0987	R_1 = 0.0376 wR_2 = 0.0785	R_1 = 0.0376 wR_2 = 0.0877	R_1 = 0.0540 wR_2 = 0.1132	R_1 = 0.0602 wR_2 = 0.1622	R_1 = 0.0445 wR_2 = 0.1099	R_1 = 0.0351 wR_2 = 0.0922	R_1 = 0.0355 wR_2 = 0.0832
R^a indices (all data)	R_1 = 0.0469 R_2 = 0.1121	R_1 = 0.0396 wR_2 = 0.0856	R_1 = 0.0429 wR_2 = 0.1030	R_1 = 0.0426 wR_2 = 0.0822	R_1 = 0.0410 wR_2 = 0.0902	R_1 = 0.0753 wR_2 = 0.1268	R_1 = 0.0752 wR_2 = 0.1793	R_1 = 0.0525 wR_2 = 0.1166	R_1 = 0.0365 wR_2 = 0.0937	R_1 = 0.0420 wR_2 = 0.0871
GOF^b	1.061	1.084	1.078	1.051	1.096	1.080	1.087	1.083	1.043	1.095
final diff peaks, e/Å^3	+0.409, −0.702	+0.877, −0.761	+1.170, −0.943	+1.192, −1.165	+1.169, −1.298	+1.003, −0.348	+0.699, −0.561	+0.601, −0.662	+0.775, −0.463	+0.707, −0.572

^{a} $R_1 = \sum||F_o| - |F_c||/\sum|F_o|$; $wR_2 = \{\sum w(F_o^2 - F_c^2)^2/\sum w(F_o^2)^2\}^{1/2}$. ^{b} GOF $= \{\sum w(F_o^2 - F_c^2)^2/(n - p)\}^{1/2}$ where n = no. of reflns; p = no. of params refined.

1803 (m, br), 1755 (w), 1721 (w, br), 1581 (m), 1497 (s), 1447 (s), 1425 (s), 1310 (m), 1212 (m), 1111 (s, br).

Alternatively, the reaction of **2** (500 mg, 1.6 mmol), $AlCl_3$ (42 mg, 0.31 mmol), and ICl (3.1 mL of a 1.0 M CH_2Cl_2 solution) in 40 mL of CS_2 for 67 h at room temperature, following the same workup as above, resulted in an increased yield of **5** (402 mg, 0.90 mmol, 58%), recovery of 86 mg of **2** (0.27 mmol, 17%), and formation of only trace amounts of **6** and **7**.

1-(η^5-C_5H_5)-2-Ph-6-(PhC≡C)-*closo*-1,2,3,4-$FeC_3B_7H_8$ (8). A diethylamine (10 mL) solution of **5** (100 mg, 0.22 mmol), bis(benzonitrile)palladium(II) chloride (9 mg, 0.022 mmol), triphenylphosphine (12 mg, 0.045 mmol), copper(I) iodide (4 mg, 0.022 mmol), and phenylacetylene (0.12 mL, 1.1 mmol) was stirred under nitrogen at room temperature for 20 h. The solvent was then removed *in vacuo*, and the resulting residue was chromatographed on TLC plates (2:1, hexanes/CH_2Cl_2) to give a dark blue band (R_f 0.38). For **8**: 1-(η^5-C_5H_5)-2-Ph-6-(PhC≡C)-*closo*-1,2,3,4-$FeC_3B_7H_8$, 37% yield (35 mg, 0.08 mmol); dark blue; mp 181 °C. Anal. Calcd: C, 63.07, H, 5.53. Found: C, 61.94, H, 5.61. HRMS: *m/z* calcd for $^{12}C_{22}{}^{1}H_{23}{}^{11}B_7{}^{56}Fe^-$ 420.1801, found 420.1813. ^{11}B NMR (128.4 MHz, CD_2Cl_2, ppm, J = Hz): 3.9 (d, 151, 1B), −0.5 (d, 153, 1B), −10.2 (d, 153, 1B), −12.9 (s, 1B), −25.6 (d, 144, 1B), −28.0 (d, 158, 1B), −34.7 (d, 160, 1B). ^{1}H NMR (400.1 MHz, CD_2Cl_2, ppm, J = Hz): 7.26−8.64 (Ph), 6.92 (dd (6, 5), C3H), 4.53 (s, Cp), 1.86 (s, C4H). IR (KBr, cm^{-1}) 3103 (s), 3088 (m), 3053 (m), 2963 (m), 2595 (vs, br), 2167 (s), 1978 (w), 1963 (m), 1890 (w), 1724 (w, br), 1678 (w), 1594 (s), 1576 (m), 1489 (s), 1445 (s), 1424 (m), 1312 (w), 1262 (s, br), 1200 (m), 1180 (m), 1138 (s), 1098 (m, br).

1-(η^5-C_5H_5)-2-Ph-6-((CH$_3$)$_3$SiC≡C)-*closo*-1,2,3,4-$FeC_3B_7H_8$(9). A diethylamine (15 mL) solution of **5** (228 mg, 0.51 mmol), bis(triphenylphosphine)palladium(II) chloride (36 mg, 0.051 mmol), copper(I) iodide (10 mg, 0.051 mmol), and (trimethylsilyl)acetylene (0.15 mL, 1.0 mmol) was stirred under nitrogen at room temperature for 22 h. The solvent was then removed *in vacuo*, and the resulting residue was chromatographed on TLC plates (2:1, hexanes/CH_2Cl_2) to give a dark blue band (R_f 0.49). For **9**: 1-(η^5-C_5H_5)-2-Ph-6-((CH$_3$)$_3$SiC≡C)-*closo*-1,2,3,4-$FeC_3B_7H_8$, 78% yield (166 mg, 0.40 mmol); dark blue; mp 154 °C. HRMS: *m/z* calcd for $^{12}C_{19}{}^{1}H_{27}{}^{11}B_7{}^{56}Fe^{28}Si^-$ 416.1883, found 416.1885. ^{11}B NMR (128.4 MHz, CD_2Cl_2, ppm, J = Hz): 3.7 (d, 163, 1B), −0.5 (d, 173, 1B), −10.0 (d, 144, 1B), −13.5 (s, 1B), −25.8 (d, 145, 1B), −28.0 (d, 168, 1B), −34.9 (d, 161, 1B). ^{1}H NMR (400.1 MHz, CD_2Cl_2, ppm, J = Hz): 7.46−8.61 (Ph), 6.85 (dd (6, 4), C3H), 4.47 (s, Cp), 1.81 (s, C4H), 0.13 (s, Me). IR (KBr, cm^{-1}): 3095 (s), 3060 (s), 3032 (m), 2958 (s), 2896 (s), 2561 (vs, br), 2125 (s), 1944 (w), 1797 (w, br), 1594 (m), 1495 (s), 1445 (s), 1424 (s), 1311 (m), 1245 (s), 1160 (s), 1094 (m), 1046 (s), 1012 (s).

1-(η^5-C_5H_5)-2-Ph-6-(HC≡C)-*closo*-1,2,3,4-$FeC_3B_7H_8$ (10). A THF (10 mL) solution of **9** (166 mg, 0.40 mmol) and tetrabutylammonium fluoride hydrate (112 mg, 0.40 mmol) was stirred under nitrogen at room temperature for 17 h. The solvent was then removed *in vacuo*, and the resulting residue was washed on a silica gel column with 100% hexanes followed by 3:1 hexanes/CH_2Cl_2 to elute a dark blue band. For **10**: 1-(η^5-C_5H_5)-2-Ph-6-(HC≡C)-*closo*-1,2,3,4-$FeC_3B_7H_8$, 68% yield (93 mg, 0.27 mmol); dark blue; mp 191 °C. Anal. Calcd: C, 56.05, H, 5.59. Found: C, 55.89, H, 5.45. HRMS: *m/z* calcd for $^{12}C_{16}{}^{1}H_{19}{}^{11}B_7{}^{56}Fe^-$ 344.1488, found 344.1508. ^{11}B NMR (128.4 MHz, CD_2Cl_2, ppm, J = Hz): 3.8 (d, 161, 1B), −0.4 (d, 174, 1B), −10.3 (d, 142, 1B), −13.6 (s, 1B), −25.6 (d, 142, 1B), −28.0 (d, 150, 1B), −34.6 (d, 155, 1B). ^{1}H NMR (400.1 MHz, CD_2Cl_2, ppm, J = Hz): 7.46−8.59 (Ph), 6.86 (dd (6, 5), C3H), 4.50 (s, Cp), 2.27 (s, -C'C-*H*), 1.82 (s, C4H). IR (KBr, cm^{-1}): 3294 (vs), 3106 (m), 3060 (m), 2920 (s), 2846 (s), 2594 (vs), 2556 (vs), 2068 (m), 1950 (w), 1883 (w), 1804 (w), 1717 (m, br), 1662 (w, br), 1595 (m), 1495 (m), 1446 (m), 1423 (m), 1315 (m), 1286 (m, br), 1153 (m), 1097 (m), 1003 (m).

1-(η^5-C_5H_5)-2-Ph-6-[$CH_3CH_2C(O)OCH_2C$≡C]-*closo*-1,2,3,4-$FeC_3B_7H_8$(11). A diethylamine (10 mL) solution of **5** (100 mg, 0.22 mmol), bis(benzonitrile)palladium(II) chloride (34 mg, 0.090 mmol), triphenylphosphine (47 mg, 0.18 mmol), copper(I) iodide (17 mg, 0.090 mmol), and propargyl propionate (0.13 mL, 1.1 mmol) was stirred under nitrogen at room temperature for 39 h. The solvent was removed *in vacuo*, and the resulting residue was chromatographed on TLC plates (100% CH_2Cl_2) to give a dark blue band (R_f 0.72). For **11**: 1-(η^5-C_5H_5)-2-Ph-6-[$CH_3CH_2C(O)OCH_2C$≡C]-*closo*-1,2,3,4-$FeC_3B_7H_8$, 32% yield (31 mg, 0.072 mmol); dark blue; mp 184 °C. Anal. Calcd: C, 56.00, H, 5.87. Found: C, 55.84, H, 5.52. HRMS: *m/z* calcd for $^{12}C_{20}{}^{1}H_{25}{}^{11}B_7{}^{56}Fe^{16}O_2^-$ 430.1855, found 430.1844. ^{11}B NMR (128.4 MHz, CD_2Cl_2, ppm, J = Hz): 3.7 (d, 150, 1B), −0.4 (d, 130, 1B), −10.3 (d, 141, 1B), −13.5 (s, 1B), −25.7 (d, 146, 1B), −28.0 (d, 161, 1B), −34.6 (d, 155, 1B). ^{1}H NMR (400.1 MHz, CD_2Cl_2, ppm, J = Hz): 7.47−8.60 (Ph), 6.85 (dd (6, 5), C3H), 4.62 (s, −C≡C−C*H*$_2$−O), 4.49 (s, Cp), 2.34 (q, 7.5, −C(O)−C*H*$_2$−CH$_3$), 1.83 (d, C4H), 1.12 (t, 7.5, −CH$_2$−C*H*$_3$). IR (KBr, cm^{-1}): 3108 (s), 2989 (m), 2942 (m), 2623 (s), 2552 (vs), 1730 (vs, br), 1597 (m), 1579 (m), 1495 (m), 1424 (m), 1372 (m), 1337 (m), 1258 (m), 1175 (s, br), 1085 (m), 1033 (w), 1003 (m).

1-(η^5-C_5H_5)-2-Ph-6-[(η^5-C_5H_5)Fe(η^5-C_5H_4)-C≡C]-*closo*-1,2,3,4-$FeC_3B_7H_8$(12). A diethylamine (10 mL) solution of **5** (115 mg, 0.26 mmol), bis(benzonitrile)palladium(II) chloride (10 mg, 0.026 mmol), triphenylphosphine (14 mg, 0.052 mmol), copper(I) iodide (5 mg, 0.026 mmol), and ethynylferrocene (109 mg, 0.52 mmol) was stirred under nitrogen at room temperature for 44 h. The solvent was removed *in vacuo*, and the resulting residue was chromatographed on TLC plates (1:1, hexanes/CH_2Cl_2) to give a dark green band (R_f 0.69). For **12**: 1-(η^5-C_5H_5)-2-Ph-6-[(η^5-C_5H_5)Fe(η^5-C_5H_4)-C≡C]-*closo*-1,2,3,4-$FeC_3B_7H_8$, 21% yield (28 mg, 0.053 mmol); dark green; mp 206 °C; Anal. Calcd: C, 59.27, H, 5.18. Found: C, 58.99, H, 5.20. HRMS: *m/z* calcd for $^{12}C_{26}{}^{1}H_{27}{}^{11}B_7{}^{56}Fe_2^-$ 528.1463, found 528.1463. ^{11}B NMR (128.4 MHz, CD_2Cl_2, ppm, J = Hz): 4.0 (d, 160, 1B), −0.5 (d, 131, 1B), −9.9 (d, 143, 1B), −12.4 (s, 1B), −25.5 (d, 142, 1B), −28.1 (d, 148, 1B), −35.0 (d, 160, 1B). ^{1}H NMR (400.1 MHz, CD_2Cl_2, ppm, J = Hz): 7.47−8.64 (Ph), 6.88 (dd (7, 4), C3H), 4.13−4.51 (Cp) 1.83 (s, C4H). IR (KBr, cm^{-1}): 3099 (s), 2924 (s), 2852 (m), 2605 (vs), 2569 (vs), 2175 (vs), 1723 (m, br), 1579 (m), 1497 (m), 1445 (m), 1419 (m), 1267 (s), 1150 (m), 1106 (m), 1055 (m), 1002 (m).

Crystallographic Data. Single crystals of compounds **3** through **12** were grown via slow solvent evaporation from dichloromethane solutions in air.

Collection and Reduction of the Data. Crystallographic data and structure refinement information are summarized in Table 1. X-ray intensity data for **3** (Penn3275), **4** (Penn3278), **5** (Penn3276), **6** (Penn3287), **7** (Penn3286), **8** (Penn3284), **9** (Penn3293), **10** (Penn3288), **11** (Penn3291), and **12** (Penn3285) were collected on a Rigaku R-AXIS IIC area detector employing graphite-monochromated Mo Kα radiation. Indexing was performed from a series of 12 0.5° rotation images with exposures of 30 s and a 36 mm crystal-to-detector distance. Oscillation images were processed using CrystalClear,[7] producing a list of unaveraged F^2 and $\sigma(F^2)$ values, which were then passed to the CrystalStructure[8] program package for further processing and structure solution on a Dell Pentium III computer. The intensity data were corrected for Lorentz and polarization effects and for absorption.

Solution and Refinement of the Structures. The structures were solved by direct methods (SIR97[9]). Refinement was by full-matrix

(7) *CrystalClear*; Rigaku Corporation, 1999.

(8) *CrystalStructure*, Crystal Structure Analysis Package; Rigaku Corp. Rigaku/MSC, 2002.

(9) *SIR97*: Altomare, A.; Burla, M. C.; Camalli, M.; Cascarano, M.; Giacovazzo, C.; Guagliardi, A.; Moliterni, A.; Polidori, G. J.; Spagna, R. *J. Appl. Crystallogr.* **1999**, *32*, 115–119.

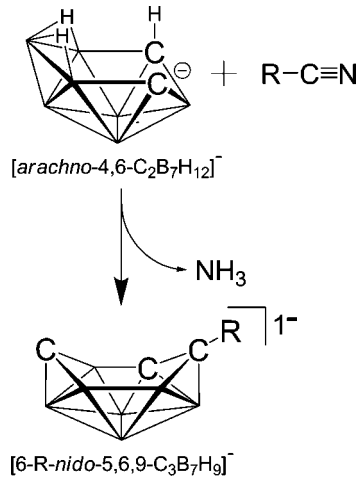

Figure 2. Syntheses of tricarbadecaboranyl ligands, [6-R-*nido*-5,6,9-$C_3B_7H_9$]$^-$, via the reaction of [*arachno*-4,6-$C_2B_7H_{12}$]$^-$ with a nitrile.

least-squares based on F^2 using SHELXL-97.[10] All reflections were used during refinement (values of F^2 that were experimentally negative were replaced with $F^2 = 0$).

Results and Discussion

Metallocenes are commonly functionalized via reactions on the coordinated cyclopentadienyl rings with both metalation and electrophilic substitution reactions giving the corresponding substituted metallocenes in excellent yields and selectivities.[11] However, we found that cyclopentadienyliron tricarbadecaboranyl complexes either are unreactive or undergo side reactions when these functionalization methods directed at the cyclopentadienyl ligand are employed. A limited number of cage-carbon-functionalized tricarbadecaboranyl anions 6-R-5,6,9-*nido*-$C_3B_7H_9^-$ (R = Me, Ph, $NC(CH_2)_4$, (*p*-BrC_6H_4)(Me_3SiO)CH, $C_{14}H_{11}$, $H_3BNMe_2(CH_2)_2$) have been produced[3h] via the reaction of a substituted nitrile RCN with the [*arachno*-4,6-$C_2B_7H_{12}$]$^-$ anion (Figure 2). Subsequent reactions of these anions with (η^5-C_5H_5)$Fe(CO)_2I$ then yielded the corresponding cage-carbon-substituted metallatricarbadecaboranyl complexes 1-(η^5-C_5H_5)-2-R-*closo*-1,2,3,4-$FeC_3B_7H_9$. Unfortunately, the further utilization of this method is limited by its functional group intolerance, the unavailability or unreactivity of the needed nitrile-containing reagent for ligand synthesis, and the low to moderate yields in both the ligand synthesis and subsequent coordination reactions.

Hawthorne and co-workers[12a,b] have reported the syntheses of a number of acetylene-functionalized *p*-carborane derivatives involving the palladium-catalyzed Sonogashira coupling reactions of iodinated *p*-carborane complexes. Utilizing a similar procedure, Grimes and co-workers[12c] achieved the linkage of $Cp^*Co(Et_2C_2B_3H_5)$ sandwiches with an acetylene spacer. As described below, the strategy of selective cage-halogenation followed by Sonogashira coupling reactions has likewise proven to be especially effective in providing general, high-yield routes to a variety of boron-functionalized cyclopentadienyliron tricarbadecaboranyl complexes.

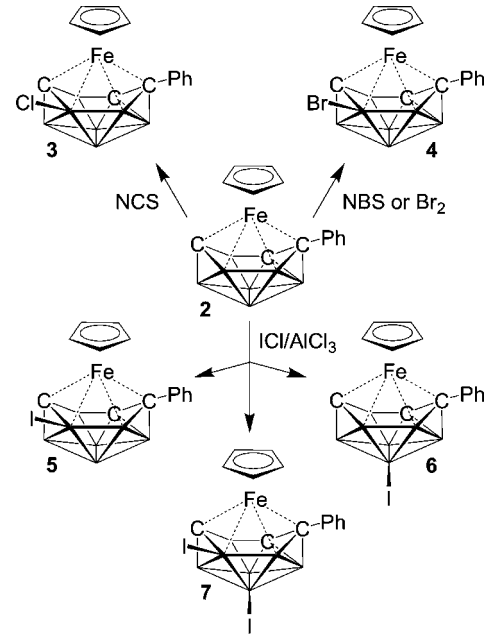

Figure 3. Halogenation reactions of **2**.

Halogenation of 1-(η^5-C_5H_5)-2-Ph-*closo*-1,2,3,4-$FeC_3B_7H_9$. The reaction of **2** with *N*-chloro- (NCS) or *N*-bromosuccinimide (NBS) resulted in selective halogenation at the B6-boron of the carborane cage to give 1-(η^5-C_5H_5)-2-Ph-6-X-*closo*-1,2,3,4-$FeC_3B_7H_8$ [X = Cl (**3**), Br (**4**)] in 52% and 95% yields, respectively (Figure 3). Alternatively, **4** was prepared by the reaction of **2** with Br_2 in only 5 min (compared to the 18 h required for the reaction of **2** with NBS), but with a lower yield of 81%. **3** and **4** were easily separated in pure form by column chromatography.

N-Iodosuccinimide (NIS) and I_2 showed no reactivity with **2**. However, the $AlCl_3$-catalyzed reaction of **2** with ICl gave not only 1-(η^5-C_5H_5)-2-Ph-6-I-*closo*-1,2,3,4-$FeC_3B_7H_8$ (**5**) but also 1-(η^5-C_5H_5)-2-Ph-11-I-*closo*-1,2,3,4-$FeC_3B_7H_8$ (**6**) and the dihalogenated product 1-(η^5-C_5H_5)-2-Ph-6-I-11-I-*closo*-1,2,3,4-$FeC_3B_7H_7$ (**7**) in 44%, 8%, and 11% yields, respectively (Figure 3). **5**, **6**, and **7** were then easily separated from each other and unreacted **2** by column chromatography. When the amounts of $AlCl_3$ and ICl relative to **2** were reduced to only 0.2 equiv of $AlCl_3$ and 2 equiv of ICl, an increased yield of **5** (58%) was obtained accompanied by a reduction in the formation of **6**and **7**.

3−**7** are air- and moisture-stable solids that are soluble in a wide variety of both polar and nonpolar organic solvents. As shown in examples in Figure 4, the ^{11}B NMR spectra of **3**−**7**, like **2**, indicate C_1 cage symmetry, showing seven resonances at chemical shifts similar to those observed for other *closo*-1,2,3,4-$MC_3B_7H_9$ cluster systems.[3] The ^{1}H-coupled ^{11}B NMR spectra of **3**−**6** show one singlet, while **7** has two singlets, consistent with halide substitution at their B6 (**3**−**5**), B11 (**6**), or B6 and B11 (**7**) borons, respectively (Figure 4). As expected, the chemical shift of the B6 boron varies according to the substituted halogen (B6: **3** (Cl), −0.9 ppm; **4** (Br), −6.8 ppm; **5** (I), −21.6 ppm) with the upfield progression consistent with the decreasing electronegativity of the halogen. The ^{1}H NMR spectra of **3**−**7** each show two cage C−H resonances; one occurring at a higher-field shift (1.79 to 2.01 ppm) characteristic

(10) Sheldrick, G. M. *SHELXL-97, Program for the Refinement of Crystal Structures*; University of Göttingen: Germany, 1997.

(11) *Comprehensive Organometallic Chemistry*; Wilkinson, G., Stone, F. G. A., Abel, E. W., Eds.; Pergamon Press: Elmsford, NY, 1982; Vol. 4, pp 475−480.

(12) (a) Jiang, W.; Knobler, C. B.; Curtis, C. E.; Mortimer, M. D.; Hawthorne, M. F. *Inorg. Chem.* **1995**, *34*, 3491–3498. (b) Jiang, W.; Harwell, D. E.; Mortimer, M. D.; Knobler, C. B.; Hawthorne, M. F. *Inorg. Chem.* **1996**, *35*, 4355–4359. (c) Malaba, D.; Sabat, M.; Grimes, R. N. *Eur. J. Inorg. Chem.* **2001**, *255*, 7–2562. (d) Russell, J. M.; Sabat, M.; Grimes, R. N. *Organometallics* **2002**, *21*, 4113–4128. (e) Beletskaya, I. P.; Brgadze, V. I.; Ivushkin, V. A.; Zhigareva, G. G.; Petrovskii, P. V.; Sivaev, I. B. *Russ. J. Org. Chem.* **2005**, *41*, 1359–1366.

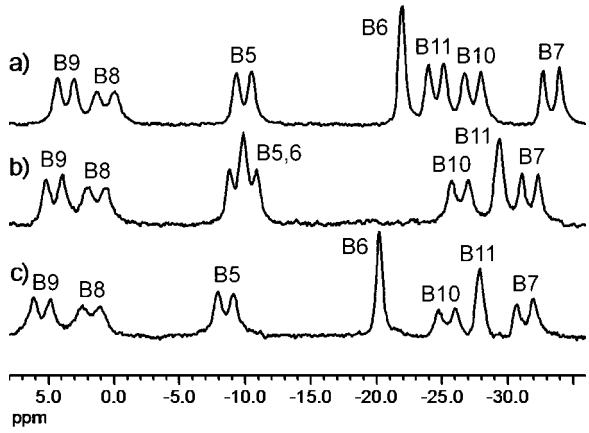

Figure 4. Comparisons of the ^{11}B NMR (128.4 MHz) spectra of (a) 1-(η^5-C_5H_5)-2-Ph-6-I-*closo*-1,2,3,4-$FeC_3B_7H_8$ (**5**), (b) 1-(η^5-C_5H_5)-2-Ph-11-I-*closo*-1,2,3,4-$FeC_3B_7H_8$ (**6**), and (c) 1-(η^5-C_5H_5)-2-Ph-6-I-11-I-*closo*-1,2,3,4-$FeC_3B_7H_8$ (**7**).

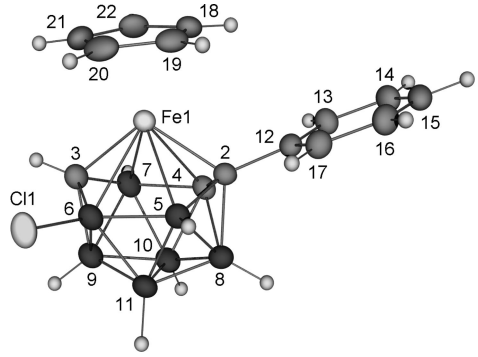

Figure 5. ORTEP representation of 1-(η^5-C_5H_5)-2-Ph-6-Cl-*closo*-1,2,3,4-$FeC_3B_7H_8$ (**3**). Selected distances (Å) and angles (deg): Fe1−C2, 1.974(2); Fe1−C3, 1.966(2); Fe1−C4, 2.243(2); Fe1−B5, 2.237(2); Fe1−B6, 2.232(2); Fe1−B7, 2.263(2); C2−C12, 1.492(3); C2−B5, 1.599(3); B5−B6, 1.839(3); C3−B6, 1.572(3); C3−B7, 1.569(3); C4−B7, 1.745(3); C2−C4, 1.499(3); Fe−$Cp_{Centroid}$, 1.684(1); B6−Cl1, 1.815(2); Fe1−C2−C12, 125.8(1); C2−Fe1−C3, 111.5(1); Cp/B5−B6−B7, 2(2).

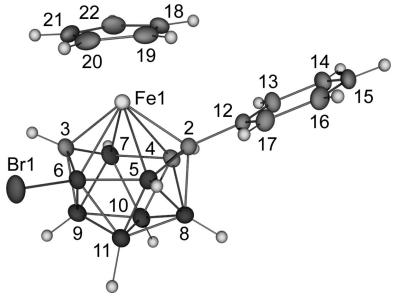

Figure 6. ORTEP representation of 1-(η^5-C_5H_5)-2-Ph-6-Br-*closo*-1,2,3,4-$FeC_3B_7H_8$ (**4**). Selected distances (Å) and angles (deg): Fe1−C2, 1.980(2); Fe1−C3, 1.966(2); Fe1−C4, 2.244(3); Fe1−B5, 2.242(3); Fe1−B6, 2.219(3); Fe1−B7, 2.270(3); C2−C12, 1.498(3); C2−B5, 1.597(3); B5−B6, 1.833(4); C3−B6, 1.572(3); C3−B7, 1.579(4); C4−B7, 1.743(3); C2−C4, 1.502(3); Fe−$Cp_{Centroid}$, 1.686(1); B6−Br1, 1.980(3); Fe1−C2−C12, 124.8(2); C2−Fe1−C3, 111.5(1); Cp/B5−B6−B7, 2(3).

of a proton attached to the C4 cage atom and the other at a lower-field shift (6.77 to 6.99 ppm) characteristic of a proton attached to a low-coordinate carbon adjacent to the metal (C3H).[3] Additionally, the C3H protons display a doublet of doublet coupling pattern for compounds **3**, **4**, **5**, and **7** and a

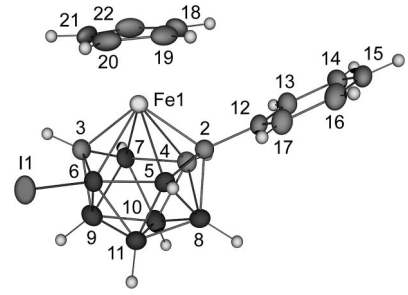

Figure 7. ORTEP representation of 1-(η^5-C_5H_5)-2-Ph-6-I-*closo*-1,2,3,4-$FeC_3B_7H_8$ (**5**). Selected distances (Å) and angles (deg): Fe1−C2, 1.974(3); Fe1−C3, 1.967(3); Fe1−C4, 2.242(3); Fe1−B5, 2.250(3); Fe1−B6, 2.223(3); Fe1−B7, 2.279(4); C2−C12, 1.499(4); C2−B5, 1.596(4); B5−B6, 1.829(5); C3−B6, 1.578(5); C3−B7, 1.591(5); C4−B7, 1.739(5); C2−C4, 1.500(4); Fe−$Cp_{Centroid}$, 1.688(1); B6−I1, 2.187(3); Fe1−C2−C12, 123.9(2); C2−Fe1−C3, 111.3(1); Cp/B5−B6−B7, 2(4).

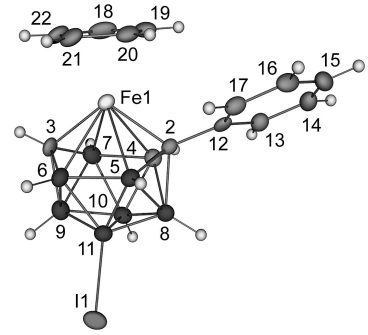

Figure 8. ORTEP representation of 1-(η^5-C_5H_5)-2-Ph-11-I-*closo*-1,2,3,4-$FeC_3B_7H_8$ (**6**). Selected distances (Å) and angles (deg): Fe1−C2, 1.979(3); Fe1−C3, 1.976(3); Fe1−C4, 2.206(3); Fe1−B5, 2.276(4); Fe1−B6, 2.275(4); Fe1−B7, 2.235(4); C2−C12, 1.506(5); C2−B5, 1.586(5); B5−B6, 1.848(5); C3−B6, 1.579(5); C3−B7, 1.557(5); C4−B7, 1.767(5); C2−C4, 1.510(4); Fe−$Cp_{Centroid}$, 1.690(1); B11−I1, 2.193(4); Fe1−C2−C12, 125.3(2); C2−Fe1−C3, 111.3(1); Cp/B5−B6−B7, 2(4).

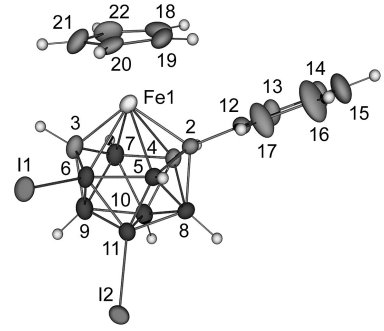

Figure 9. ORTEP representation of 1-(η^5-C_5H_5)-2-Ph-6-I-11-I-*closo*-1,2,3,4-$FeC_3B_7H_7$ (**7**). Selected distances (Å) and angles (deg): Fe1−C2, 1.980(4); Fe1−C3, 1.969(5); Fe1−C4, 2.261(4); Fe1−B5, 2.237(4); Fe1−B6, 2.231(4); Fe1−B7, 2.290(5); C2−C12, 1.493(5); C2−B5, 1.596(5); B5−B6, 1.845(6); C3−B6, 1.572(6); C3−B7, 1.588(6); C4−B7, 1.735(6); C2−C4, 1.510(5); Fe−$Cp_{Centroid}$, 1.713(1); B6−I1, 2.172(4); B11−I2, 2.183(4); Fe1−C2−C12, 126.3(3); C2−Fe1−C3, 111.0(2); Cp/B5−B6−B7, 3(6).

multiplet pattern for **6** owing to couplings to the adjacent BH protons (i.e., to B7H and B9H in **3**, **4**, **5**, and **7** and to B7H, B9H, and B10H in **6**). The C3H resonance for **3**−**5** also shifts to higher field as the halogen electronegativity decreases (**3**, 6.77 ppm; **4**, 6.90 ppm; **5**, 6.99 ppm). This trend contrasts with the relatively constant C4H chemical shift values.

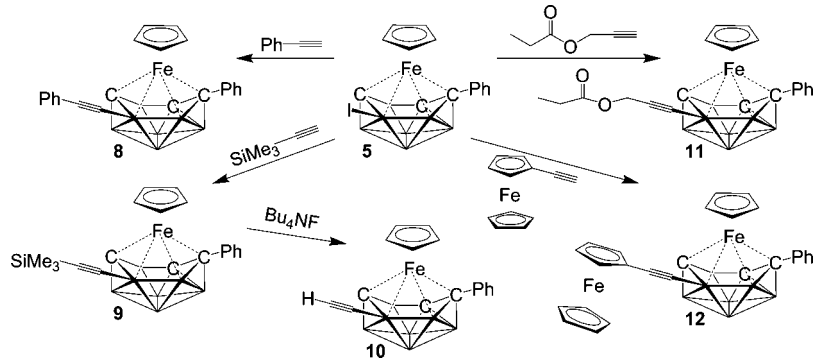

Figure 10. Sonogashira coupling reactions of **5** with 20% $(PPh_3)_2PdCl_2$/CuI in NEt_2H.

In agreement with the spectroscopic data and the predicted *closo*-electron count of their $MC_3B_7H_9$ fragments (24 skeletal electrons), crystallographic determinations of **3**−**7** confirmed that the metallatricarbadecaboranyl cages adopt octadecahedral geometries (Figures 5−9) with the metal η^6-coordinated to, and approximately centered over, the puckered six-membered face of the tricarbadecaboranyl cage. **3**, **4**, **5**, and **7** have statistically equivalent Fe−cage and intercage distances, but **6** shows slightly elongated Fe−B5 and Fe−B6 distances (2.276(4) and 2.275(4) Å) and shortened Fe−C4 and Fe−B7 distances (2.206(3) and 2.235(4) Å) compared with the average distances observed in **3**, **4**, **5**, and **7** (Fe−B5, 2.242(3) Å; Fe−B6, 2.227(3) Å; Fe−C4, 2.247(3) Å; Fe−B7, 2.275(3) Å). In addition, the C3−B7 distance (1.557(5) Å) is shorter and the C4−B7 distance (1.767(5) Å) is longer in **6** than the average distances in **3**, **4**, **5**, and **7** (1.582(5) and 1.740(4) Å, respectively). The respective B6−Cl1 (1.815(2) Å), B6−Br1 (1.980(3) Å), and B6−I1 (2.187(3) Å) distances in **3**−**5** are all consistent with those of other halogenated metallacarboranes.[13]

Regardless of the halogen or reaction conditions employed, **2** halogenation was observed at only the B6 and B11 cage positions, with a strong preference for substitution at B6. This is consistent with the known preference for cage-halogenations in metallacarboranes at boron positions that are adjacent to the metal center (i.e., B6 in **2**) and those furthest separated (i.e., both B6 and B11 in **2**) from the cage-carbons.[14] For example, Plešek and co-workers[15] found that the order of the stepwise halogenation of Cs[*commo*-3,3′-Co(1,2-$C_2B_9H_{11})_2$] was B8 > B9 > B12, where the B8 position is adjacent to the metal center with no neighboring carbon atoms and the B9 and B12 positions are opposite the cage-carbons.

Palladium-Catalyzed Sonogashira Coupling Reactions. The room-temperature reaction of **5** with phenylacetylene in the presence of 20 mol % $(PPh_3)_2PdCl_2$/CuI using diethylamine as both a base and solvent afforded the acetylene-functionalized product 1-(η^5-C_5H_5)-2-Ph-6-(PhC≡C)-*closo*-1,2,3,4-$FeC_3B_7H_8$ (**8**) in 37% yield. Using these conditions, acetylene derivatives containing terminal trimethylsilane (**9**), ester (**11**), and ferrocene (**12**) functional groups were obtained (Figure 10). For each reaction, only a single product was observed.

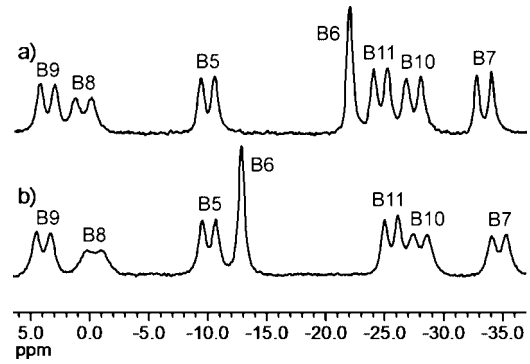

Figure 11. Comparison of the ^{11}B NMR (128.4 MHz) spectra of (a) 1-(η^5-C_5H_5)-2-Ph-6-I-*closo*-1,2,3,4-$FeC_3B_7H_8$ (**5**) and (b) 1-(η^5-C_5H_5)-2-Ph-6-(PhC≡C)-*closo*-1,2,3,4-$FeC_3B_7H_8$ (**8**).

8−**12** were easily isolated following column chromatography as air- and moisture-stable blue solids, which were soluble in a wide variety of both polar and nonpolar organic solvents.

Treatment of **9** with tetrabutylammonium fluoride hydrate resulted in the straightforward removal of the trimethylsilyl group (eq 1) to give the terminal, unsubstituted ethynyl metallacarborane complex in 68% yield.

$$(\mathbf{9}) + Bu_4N^+F^-\cdot H_2O \rightarrow 1\text{-}(\eta^5\text{-}C_5H_5)\text{-}2\text{-Ph-}6\text{-}(HC{\equiv}C)\text{-}closo\text{-}1,2,3,4\text{-}FeC_3B_7H_8\ (\mathbf{10}) + (CH_3)_3SiF + Bu_4N^+OH^- \quad (1)$$

$Bu_4N^+F^-$ has previously been utilized as a deboronation reagent, but no deboronation was observed during the deprotection reaction.

Replacement of iodine by an acetylene group caused the B6 singlet resonance in the proton-coupled ^{11}B NMR spectra of **8**−**12** to shift downfield from −22 ppm in **5** (Figure 11a) to −13−14 ppm in **8**−**12** (Figure 11b), but the B6 chemical shift was essentially unaffected by the terminal functionality of the acetylene linker. As for **3**−**7**, the ^1H NMR spectra of **8**−**12** each show two cage C−H resonances, one occurring at a higher-field shift (1.80−1.86 ppm) characteristic of a proton attached to the C4 cage atom and the other at a lower-field shift (6.85−6.92 ppm) characteristic of a proton attached to a low-coordinate carbon adjacent to the metal (C3H).[3] Likewise, C3H displays a doublet of doublets coupling pattern owing to its coupling to the adjacent BH protons (i.e., B7H and B9H). Unlike **3**−**5**, the chemical shift of the C3H resonance for **8**−**12** did not vary with the substituent attached to the acetylene group. The other observed ^1H resonances are those expected for the substituted functional groups and are similar to those of the acetylenic starting materials.

(13) (a) Hurlburt, P. K.; Miller, R. L.; Abney, K. D.; Foreman, T. M.; Butcher, R. J.; Kinkead, S. A. *Inorg. Chem.* **1995**, *34*, 5215–5219. (b) Sivý, P.; Preisinger, A.; Baumgartner, O.; Valach, F.; Koreò, B.; Mátel, L. *Acta Crystallogr.* **1986**, *C42*, 24–27. (c) Sivý, P.; Preisinger, A.; Baumgartner, O.; Valach, F.; Koreò, B.; Mátel, L. *Acta Crystallogr.* **1986**, *C42*, 28–30.

(14) Bregadze, V. I.; Timofeev, S. V.; Sivaev, I. B.; Lobanova, I. A. *Russ. Chem. Rev.* **2004**, *73*, 433–453.

(15) Mátel, L.; Macášek, F.; Rajec, P.; Heømánek, S.; Plešek, J. *Polyhedron* **1982**, *1*, 511–519.

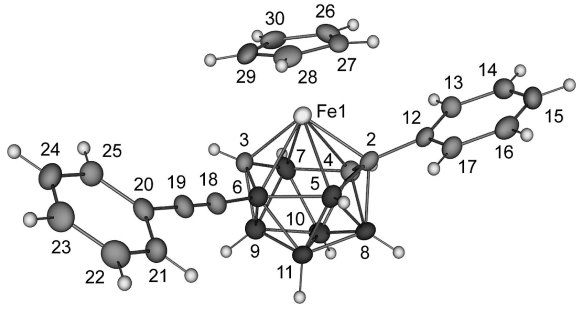

Figure 12. ORTEP representation of 1-(η^5-C_5H_5)-2-Ph-6-(PhC≡C)-*closo*-1,2,3,4-$FeC_3B_7H_8$ (**8**). Selected distances (Å) and angles (deg): Fe1−C2, 1.974(3); Fe1−C3, 1.958(4); Fe1−C4, 2.233(4); Fe1−B5, 2.252(4); Fe1−B6, 2.262(4); Fe1−B7, 2.262(4); C2−C12, 1.510(5); C2−B5, 1.576(5); B5−B6, 1.862(6); C3−B6, 1.570(6); C3−B7, 1.564(6); C4−B7, 1.758(6); C2−C4, 1.496(5); B6−C18, 1.543(5); C18−C19, 1.205(5); C19−C20, 1.442(5); Fe−$Cp_{Centroid}$, 1.681(1); Fe1−C2−C12, 125.4(2); C2−Fe1−C3, 110.9(2); Cp/B5−B6−B7, 4(2); B6−C18−C19, 176.5(4); C18−C19−C20, 178.4(4).

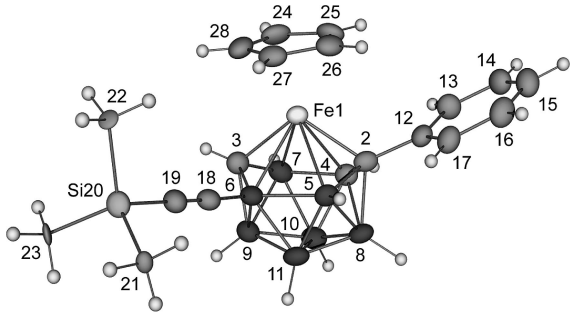

Figure 13. ORTEP representation of 1-(η^5-C_5H_5)-2-Ph-6-($(CH_3)_3SiC$≡C)-*closo*-1,2,3,4-$FeC_3B_7H_8$ (**9**). Selected distances (Å) and angles (deg): Fe1−C2, 1.978(4); Fe1−C3, 1.963(4); Fe1−C4, 2.272(4); Fe1−B5, 2.237(5); Fe1−B6, 2.232(5); Fe1−B7, 2.290(5); C2−C12, 1.493(6); C2−B5, 1.602(6); B5−B6, 1.848(7); C3−B6, 1.586(6); C3−B7, 1.566(6); C4−B7, 1.747(7); C2−C4, 1.502(6); B6−C18, 1.541(6); C18−C19, 1.210(6); C19−Si20, 1.843(4); Fe−$Cp_{Centroid}$, 1.691(1); Fe1−C2−C12, 124.3(3); C2−Fe1−C3, 110.7(2); Cp/B5−B6−B7, 5(2); B6−C18−C19, 176.4(4); C18−C19−Si20, 177.9(4).

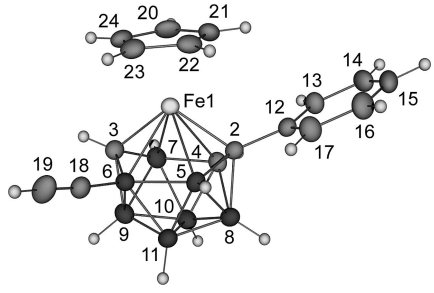

Figure 14. ORTEP representation of 1-(η^5-C_5H_5)-2-Ph-6-(HC≡C)-*closo*-1,2,3,4-$FeC_3B_7H_8$ (**10**). Selected distances (Å) and angles (deg): Fe1−C2, 1.980(2); Fe1−C3, 1.963(2); Fe1−C4, 2.265(2); Fe1−B5, 2.238(2); Fe1−B6, 2.248(2); Fe1−B7, 2.275(3); C2−C12, 1.496(3); C2−B5, 1.586(3); B5−B6, 1.861(3); C3−B6, 1.587(3); C3−B7, 1.571(4); C4−B7, 1.752(3); C2−C4, 1.501(3); B6−C18, 1.542(3); C18−C19, 1.188(3); Fe−$Cp_{Centroid}$, 1.688(1); Fe1−C2−C12, 124.4(2); C2−Fe1−C3, 111.0(1); Cp/B5−B6−B7, 4(1); B6−C18−C19, 176.7(3).

Crystallographic determinations of **8**−**12** confirm that the metallatricarbadecaboranyl cages again adopt octadecahedral geometries (Figures 12−16) with the metal η^6-coordinated to, and approximately centered over, the puckered six-membered face of the tricarbadecaboranyl cage. With the exception of the Fe−cage distances of **8**, there are no statistical differences between the Fe−cage, intercage, and B6−$C_{acetylene}$ distances in **8**−**12**. The Fe−C4 (2.233(3) Å) and Fe−B7 (2.262(4) Å) distances of **8** are slightly shorter than the average Fe−C4 (2.271(3) Å) and Fe−B7 (2.285(3) Å) distances of **9**−**12**, while the Fe−B5 (2.252(4) Å) and Fe−B6 (2.262(4) Å) distances in **8** are slightly elongated compared to the average Fe−B5 (2.234(3) Å) and Fe−B6 (2.238(3) Å) distances of **9**−**12**. The Fe−$Cp_{centroid}$ distances for **8**−**12** are consistent with those previously reported[3j] for other cyclopentadienyliron tricarbadecaboranyl complexes. Additionally, the acetylenic C−C bond of **10** (1.188(3) Å) is slightly shorter than the equivalent C−C

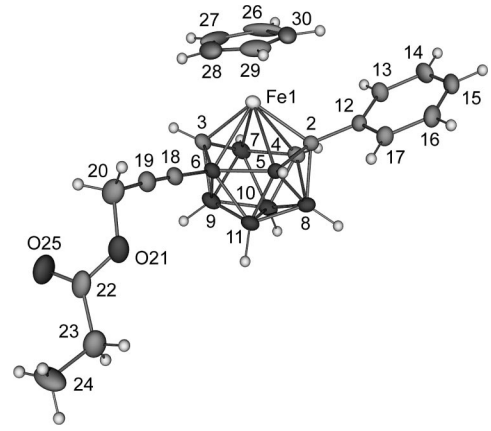

Figure 15. ORTEP representation of 1-(η^5-C_5H_5)-2-Ph-6-[$CH_3CH_2C(O)OCH_2C$≡C]-*closo*-1,2,3,4-$FeC_3B_7H_8$ (**11**). Selected distances (Å) and angles (deg): Fe1−C2, 1.986(2); Fe1−C3, 1.959(2); Fe1−C4, 2.285(2); Fe1−B5, 2.228(2); Fe1−B6, 2.230(2); Fe1−B7, 2.292(2); C2−C12, 1.494(2); C2−B5, 1.596(2); B5−B6, 1.858(2); C3−B6, 1.590(2); C3−B7, 1.577(3); C4−B7, 1.743(3); C2−C4, 1.498(2); B6−C18, 1.541(2); C18−C19, 1.197(2); C19−C20, 1.462(2); Fe−$Cp_{Centroid}$, 1.696(1); Fe1−C2−C12, 125.4(1); C2−Fe1−C3, 110.8(1); Cp/B5−B6−B7, 6.5(6); B6−C18−C19, 174.9(2); C18−C19−C20, 176.4(2).

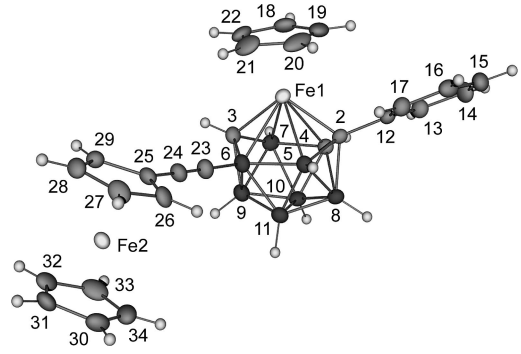

Figure 16. ORTEP representation of 1-(η^5-C_5H_5)-2-Ph-6-[(η^5-C_5H_5)Fe(η^5-C_5H_4)-C≡C]-*closo*-1,2,3,4-$FeC_3B_7H_8$ (**12**). Selected distances (Å) and angles (deg): Fe1−C2, 1.982(2); Fe1−C3, 1.967(2); Fe1−C4, 2.261(2); Fe1−B5, 2.233(2); Fe1−B6, 2.243(2); Fe1−B7, 2.282(2); C2−C12, 1.500(3); C2−B5, 1.585(3); B5−B6, 1.856(3); C3−B6, 1.583(3); C3−B7, 1.570(3); C4−B7, 1.749(3); C2−C4, 1.498(3); B6−C23, 1.538(3); C23−C24, 1.208(3); C24−C25, 1.429(3); Fe1−Cp(C18, C19, C20, C21, C22)$_{Centroid}$, 1.687(1); Fe2−Cp(C25, C26, C27, C28, C29)$_{Centroid}$, 1.647(1); Fe2−Cp(C30, C31, C32, C33, C34)$_{Centroid}$, 1.656(1); Fe1−C2−C12, 125.3(1); C2−Fe1−C3, 110.8(1); Cp(C18, C19, C20, C21, C22)/B5−B6−B7, 5.4(9); Cp(C25, C26, C27, C28, C29)/Cp(C30, C31, C32, C33, C34), 1(6); Fe1−B6−C23−C24/Cp(C25, C26, C27, C28, C29), 86.4(1); B6−C23−C24, 173.4(2); C23−C24−C25, 176.6(2).

bond in **8**, **9**, **11**, and **12** (average $C-C_{acetylene}$ 1.205(4) Å). The individual $C-C_{acetylene}$ distances are consistent with those of other analogous ethynylferrocene complexes (e.g., $Fc-C\equiv CSi(CH_3)_3$ (1.189(7) Å),[16] $Fc-C\equiv C-Fc$ (1.222(7) Å),[17] $Fc-(C\equiv CPh)_2$ (1.184(7) and 1.199(4) Å)[18]). In addition, the $B6-C_{acetylene}$ distances are consistent with those of other ethynyl-functionalized carboranes[12b] and metallacarboranes.[19] The lack of variation in the bond lengths of these complexes indicates that the terminal ethynyl functional group does not affect cage geometry or the acetylene bond.

The synthetic procedures described above, employing the selective cage-halogenation and palladium-catalyzed Sonogashira coupling steps, now provide the first general routes to boron-functionalized metallatricarbadecaboranyl complexes. The versatility and functional group tolerance of Sonogashira coupling reactions should enable the syntheses of a wide variety of derivatives with bioactive functional groups. The deprotected parent acetylene derivative **10**, when used as a reactant for additional Songashira couplings, should likewise prove to be an extremely important synthon for the construction of such complexes, and in this regard, this approach has recently been employed[20] to synthesize a 2′-deoxyadenosine derivative of **10**.

As illustrated by the synthesis of the acetylene-linked hybrid ferrocene/cyclopentadienyl-ferratricarbadecaboranyl complex **12**, these synthetic methods also have the potential to produce a wide range of new hybrid complexes with potential electron-transfer and nonlinear optical properties. Of particular interest is the construction of new metallocene-like dimetallic complexes linked by conjugated groups that enable electron transfer between the metal centers, and potential optical materials containing metallatricarbadecaboranyl complexes that are connected via conjugated linkers to electron donors or acceptors. As shown in Figure 17, **12** is, in fact, the analogue of the well-known optically active bimetallic ferrocene-based $Fc-C\equiv C-Fc$[17] complex, but because of the substantial differences in the electronic and bonding properties of the tricarbadecaboranyl and cyclopentadienyl ligands, complexes like **12** are expected to have electrochemical and optical properties that are unique from their metallocene counterparts. Compared to the corresponding metallocenes, metallatricarbadecaboranyl complexes much more readily accept electrons via chemical[3j,k] or electrochemical[3j,l] processes that are facilitated by the $\eta^6-\eta^4$ cage slippage that occurs upon reduction. For complex **2**, the one-electron reduction is a remarkable 1.74 V more favorable than that of ferrocene. Thus, in complex **12** the cyclopentadienyl ferratricarbadecaboranyl unit is the electron acceptor (the pull), while the ferrocene unit is the donor (the push). The use of synthetic methods described herein will now provide rational pathways to new classes of donor−acceptor optical and electronic materials where a metallocene or other type of electron donor can be connected through a conjugated linker to a metallatricarbdecaboranyl acceptor. We are now exploring these possibilities.

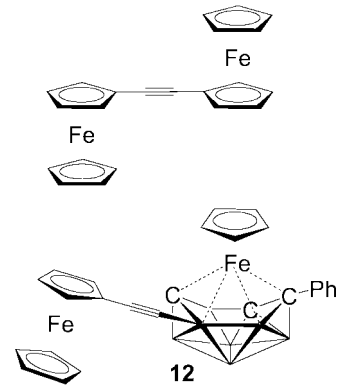

Figure 17. Comparison of $Fc-C\equiv C-Fc$ and **12**.

Acknowledgment. The National Science Foundation is gratefully acknowledged for their support of this research.

Supporting Information Available: X-ray crystallographic data for structure determinations of **3**−**12** (CIF). This material is available free of charge via the Internet at http://pubs.acs.org.

OM8003898

(16) Schottenberger, H.; Wurst, K.; Buchmeiser, M. R. *J. Organomet. Chem.* **1999**, *584*, 301–309.

(17) Kotora, M.; Neèas, D.; Štìpnièka, P. *Collect. Czech. Chem. Commun.* **2003**, *68*, 1897–1903.

(18) Ingham, S. L.; Khan, M. S.; Lewis, J.; Long, N. J.; Raithby, P. R. *J. Organomet. Chem.* **1994**, *470*, 153–159.

(19) Yao, H.; Sabat, M.; Grimes, R. N.; Zanello, P.; Fabrizi de Biani, F. *Organometallics* **2003**, *22*, 2581–2593.

(20) Olejniczak, A. B.; Butterick, R.; Sneddon, L. G.; Lesnikowski, Z. J. Presented at VIIIth Polish Organic Meeting, Lodz, Poland, April 10−12, 2008.